Nutrition 58 (2019) 156–166

Contents lists available at ScienceDirect

Nutrition

journal homepage: www.nutritionjrnl.com

Basic nutritional investigation

Excess of nutrient-induced morphofunctional adaptation and inflammation degree in a Caco2/HT-29 in vitro intestinal co-culture

Michela Bottani Ph.D. Student [a], Laura Cornaghi Post Doctor [a], Elena Donetti Assoc. Prof. [a], Anita Ferraretto Researcher [a,b,*]

[a] *Dipartimento di Scienze Biomediche per la Salute, Università degli Studi di Milano, Milano, Italy*
[b] *Centro Ricerca Metabolismi, San Donato Milanese, Italy*

ARTICLE INFO

Article History:
Received 8 June 2018
Accepted 30 July 2018

Keywords:
Excess nutrients
Caco2/HT-29 co-culture
Transmission electron microscopy
Permeability
Oxidative status
Inflammation

ABSTRACT

Objectives: The intestinal cell function can be modulated by the type and quantity of nutrients. The aim of this study was to evaluate the effects of an excess of nutrients on intestinal morphofunctional features and a possible association of inflammation in a 70/30 Caco2/HT-29 intestinal in vitro co-culture.
Methods: An excess of nutrients (EX) was obtained by progressively increasing the medium change frequency with respect to standard cell growth conditions (ST) from confluence (T0) to 15 d after confluence (T15).
Results: In comparison with the ST group, the EX group revealed a maintenance in the number of microvilli, an increase in follicle like–structures and mucus production, and a decrease in the number of tight junction. The specific activity of markers of intestinal differentiation, alkaline phosphatase and aminopeptidase N, and of the enterocyte differentiation specific marker, dipeptidyl peptidase-IV, were progressively raised. The transepithelial electrical resistance, indicative of the co-culture barrier properties, decreased, whereas Lucifer yellow P_{app} evaluation, an index of the paracellular permeability to large molecules, showed an increase. Reactive oxygen species and nitric oxide production, indicative of an oxidative status, together with interleukin-6, interleukin-8, indicative of a low-grade inflammation, and peptide YY secretion were higher in the EX group than in the ST group. The differences between ST and EX were particularly evident at T15.
Conclusion: These data support the suitability of our in vitro gut model for obesity studies at the molecular level and the necessity to standardize the medium frequency change in intestinal culture.

Introduction

The interaction between nutrients and intestinal cells consists of more than nutrient absorption and removal of harmful substances. In fact, nutrients and food components can deeply modify the intestinal cell morphology and functions, such as proliferation, differentiation, permeability, and immunologic responsiveness [1]. The modulation of intestinal cell function induced by nutrients could be due to the presence of one or more specific nutrients, the most studied interactions, and a food excess. In the latter case, the morphologic studies performed so far with in vivo studies have revealed that a diet characterized by an excess of nutrients determines the following:

- an increased number of intestinal epithelial cells [2];
- an increased proliferation rate [3];
- an increased villi length and cript depth [4,5]; and

a redistribution of zonula occluden-1 and occludin proteins with a consequent alteration in the structure and localization of the tight junctions [6].

All these morphologic modifications lead to increased intestinal absorbent surface and, as a consequence, to an augmented assimilation capacity, supported by a preferred differentiated enterocyte phenotype, associated to a decrement in both Paneth and goblet cells [3]. The functional features of the intestine in obese and overweight animals are similarly modified with the following:

- increased activity of the alkaline phosphatase (ALP), a known marker of intestine differentiation, both in the duodenum and jejunum [7];
- reduction in the dipeptidyl peptidase-IV (DPP-IV) activity [8,9];

This work was supported by the fund Piano di Sviluppo dell'Ateneo UNIMI 2016 - linea B-Ferraretto "Studio degli effetti indotti dall'eccesso di nutrienti in un modello in vitro di intestino umano costituito da una co-coltura di cellule Caco2/HT-29," Università degli Studi di Milano.
* Corresponding author: Tel.: +39 025 033 0341; Fax:
E-mail address: anita.ferraretto@unimi.it (A. Ferraretto).

https://doi.org/10.1016/j.nut.2018.07.018
0899-9007/

- increased activity of aminopeptidase N (APN) [10,11]; and
- increased circulating levels of inflammatory cytokines, interleukin (IL)-8, IL-1 β, IL-6, and tumor necrosis factor (TNF)-α [12].

Despite the results obtained using animal models, as reported previously, no data are available from in vitro intestinal cell cultures. Therefore the aim of the present study was to analyze the effects exerted by an excess of nutrients on morphofunctional adaptation and the association with low-grade inflammation in a co-culture of Caco2/HT-29 70/30 cells, which was recently characterized [13] and used for studies of nutrient absorption [14–18].

The total amount of nutrient administered to co-culture cells was considered and an excess of nutrients was realized by changing the frequency of the medium administration. Morphologic features concerning differentiation toward the different intestinal cell types and functional markers, such as enzymes and permeability, were analyzed at different postconfluence days. Reactive oxygen species (ROS) and nitric oxide (NO) generation, inflammation degree, and peptide YY (PYY) anorectic hormone production also were monitored and correlated with the above data. Results obtained can be useful to study, in a more standardized experimental plan, the molecular mechanisms responsible for the main obese phenotype features and to normalize, as much as possible, the in vitro intestinal cell growth to reproduce the human intestinal epithelium.

Materials and methods

All cell culture media and reagents were from Sigma-Aldrich (St. Louis, MO, USA). Fetal bovine serum was from EuroClone Ltd (West Yorkshire, UK).

Caco2/HT-29 cell co-culture

The co-culture was settled by culturing separately the HT-29 (BS TCL 132) and Caco2 (BS TCL 87) cell lines until their differentiation, as previously described [19,20]. After that, a mixture of 70% Caco2 from 20th to 40th passage and 30% HT-29 from 22nd to 40th passage was plated in RPMI 1640 medium, supplemented with 10% fetal bovine serum, 2 mM L-glutamine, 0.1 mg/L streptomycin, 100 000 U/L penicillin, and 0.25 mg/L amphotericin-B, containing 13.9 mM of glucose (complete RPMI), and cells were allowed to grow until day 15 of postconfluence [13]. Cells were kept at 37°C in a 5% carbon dioxide–95% air atmosphere and were periodically checked for the presence of mycoplasma. For all the experiments, a density of 40 000 cells/cm^2 was used for the seeding procedure.

Timeliness and frequency of medium change and analysis

To mimic the exposition at different nutrient amounts, three medium-change protocols (schematized in Fig 1) were applied to the co-culture:

1. Standard (ST) protocol with the amount of nutrients supplied in normal culture conditions and performed with a complete medium change every 4 d.
2. Intermediate (IN) protocol with a complete medium change alternated with only half medium change every 2 d.
3. Excess (EX) protocol with a complete medium change every 2 d.

The three protocols were applied starting from the cell confluence (T0) and the morphofunctional characteristics of the co-culture were analyzed for each protocol after 3, 7, 11, and 15 d of postconfluence (named, respectively, T3, T7, T11, T15).

Transmission electron microscopy analysis

Cells were cultured in tissue culture dishes (Grainer bio-one; Cellstar, Frickenhausen, Germany) and maintained in a complete RPMI medium until postconfluence. Cells were fixed for 60 min at room temperature (RT) with 3% glutaraldehyde buffered in 0.1 M Sorensen phosphate buffer (pH 7.4). After three washings of 30 min each with 0.1 M Sorensen phosphate buffer (pH 7.4), cells were postfixed in 1% osmium tetraoxide in the same buffer; stained with uranyl acetate 2% in water; dehydrated in 50%, 75%, 96%, 100% ethanol (three passages of 5 min each); and embedded in araldite (Durcupan; Fluka, Milan, Italy). Ultrathin sections (80 nm thick) were obtained with an Ultracut ultramicrotome (Reichert Ultracut R-Ultramicrotome; Leika, Wien, Austria), and stained with lead citrate before examination using a Jeol CX100 electron microscope (Jeol, Tokyo, Japan).

Periodic Acid-Schiff (PAS)/Alcian Blue staining

Cells were cultured in a 24-well plate (BD Falcon Cell Culture Insert PET 1 μm, BD Falcon Companion Tissue Culture Plate, Falcon Corning; Life Science, Durham, NC, USA) and maintained in complete RPMI medium. Cells were fixed in 4% paraformaldehyde diluted with 0.1 M phosphate-buffered saline (PBS) at pH 7.4 for 20 min at RT, rinsed in PBS, and placed in 70% ethanol. The membranes of the inserts were removed using forceps, then placed in lens paper, wrapped up by folding four times, placed in embedding cassettes, and replaced to 70% ethanol for 3 h on a stirrer. Samples were dehydrated using an ascending series of ethanol and paraffin embedded. Sections of 4 μm thick were cut with a microtome RM2245 (Leica Microsystems GmbH, Wetzlar, Germany).

Sections were dewaxed and rehydrated through a descending series of ethanol. After rinsing in 3% acetic acid, slides were stained with 1% Alcian blue pH 2.5 for 15 min, oxidized in 1% periodic acid for 5 min, and rinsed in distilled water. Sections were then immersed in Schiff's reagent for 5 min, rinsed in 0.5% sodium meta-bisulphate for 2 min, dehydrated through an ascending series of ethanol, and mounted with Entellan. Images were acquired using a Nikon Eclipse 80 i microscope equipped with a digital camera Nikon DS-5 Mc (Nikon, Tokyo, Japan).

Proliferation rate (Trypan blue)

The Trypan blue assay was performed to evaluate the number of living cells present in the co-culture at each time point [21]. Cells were seeded in 1 mL of complete RPMI medium in a 24-well plate (Greiner bio-one Cellstar, Italy) and allowed to grow. The day of the experiment, co-culture cells were detached with 400 μL of trypsin-EDTA from the growth support. The trypsin effect was stopped with 1 mL of complete RPMI medium. Cells were stained with trypan blue and the uncolored living ones were counted by means of a burker chamber. Results were expressed as number of living cells/cm^2 of growth support area.

Isolation of cell brush border containing fraction

Co-culture cells were seeded in 75 cm^2 flasks and, at each time point, after medium discharged, detached and collected in 9 mL of physiological saline (NaCl 0.9%, 4°C) by means of a cell scraper. Finally, cells were pelleted in a centrifuge tube (1300*g*, 4°C, Eppendorf Milan, Italy centrifuge 5810 R USA) and the supernatant was removed. According to a well-described procedure [22,23], cell extracts were obtained as follows: The cell pellet was suspended in 1 mL Tris/Mannitol buffer (Tris 2 mM-Mannitol 50 mM, pH 7.1, 4°C) and homogenized by ultrasonication (Sonoplus Ultraschall-Homogenisatoren, Bandeline, Germany). After the addition of $CaCl_2$ at final concentration of 20 mM, the cell homogenate was mixed on a rotating plate at 4°C for 10 min. At the end, samples were centrifuged twice: first, the cell homogenate at 950*g* and 4°C for 10 min (Eppendorf centrifuge 5810 R) and second, the obtained supernatants were centrifuged for 30 min at 28 000*g* and 4°C (TL-100 Beckman, Brea, CA, USA) to obtain a small pellets (P2 fraction) containing the brush border membranes. This fraction was suspended in Tris/Mannitol buffer and used for enzyme activity assays. The protein content determination of both homogenate (H) and P2 fraction was determined by the Lowry method [24].

Alkaline phosphatase assay, EC 3.1.3.1

The determination of ALP-specific activity is based on the conversion of *P*-nitrophenyl-phosphate (PNPP), colorless, in *P*-nitrophenol (PNP), with color development [25].

P2 fractions (20 μL) were solubilized in a final volume of 50 μL bi-distilled water and, at each sample, 500 μL of the reaction mixture (0.1 M sodium bicarbonate, 5 mM magnesium chloride and 7 mM PNPP) was added. At the same time, 50 μL of two PNP standard solutions (10 and 100 nmoles) were prepared and diluted with 500 μL of the previous reaction mixture devoid of PNPP. The assay was performed at 37°C in the dark. After 25 min, the reaction was stopped adding 1 mL of 0.1 M NaOH to each sample. The absorbance was measured at 410 nm and the PNP nmoles formed were calculated by means of the standard curve. The ALP-specific activity was expressed as mU/mg protein (one Unit is defined as the enzyme activity able to hydrolyses 1 μmole substrate/min)

DPP-IV assay, EC 3.4.14.5

The method used to measure the DPP-IV–specific activity was based on the release of β-naphthylamine from the DPP-IV substrate Gly-Pro β-naphthylamide [26].

P2 fraction (1 μL) was suspended in 400 μL of 50 mM Tris-HCl buffer (pH 8.4) containing 2 mM Gly-Pro β-naphthylamide. Using the same buffer, two standard solutions of β-naphthylamine (3 and 50 μM) were prepared. The prepared samples were incubated at 37°C in the dark and, after 30 min, 300 μL of 32% trichloroacetic acid was added to each tube to stop the reaction. β-naphthylamine is colorless. For this reason, 100 μL of 0.3% sodium nitrite, 100 μL of 1.5% ammonium sulfamate, and 300 μL of 0.1% *N*-1-naphthyleyhylenediamine dihydrochloride (in

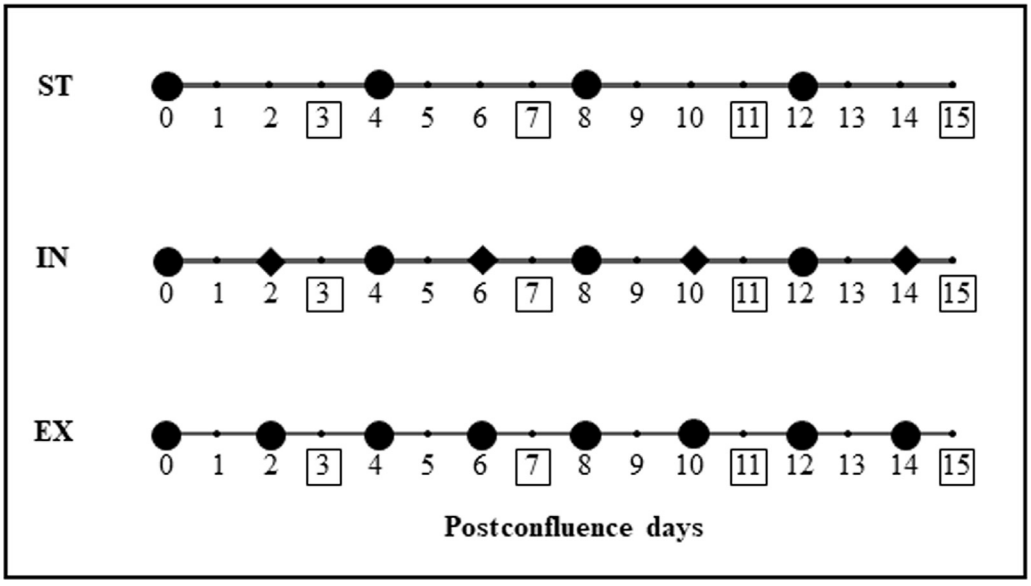

Fig. 1. Schematization of ST, IN, and EX medium-change protocols. Time axes show full medium changes in ST condition (black circles), full medium changes (black circles) + half medium changes (black rhombus) in IN condition, and full medium changes (black circles) in EX condition. Numbers in time axes represent days from the confluence (0). Number in squares mean the analyzed time points. EX, excess; IN, intermediate; ST, standard.

95% ethanol) were added in sequence to develop the color [27]. The absorbance of each sample was evaluated at 560 nm and the formed β-naphthylamine μmoles were calculated using the standard curve. The DPP-IV–specific activity was expressed as mU/mg protein.

Aminopeptidase N assay, EC 3.4.11.2

The APN-specific activity was evaluated by the chromogenic 4-Nitroaniline production from L-Ala 4-Nitroanilide, an APN substrate [28].

P2 fraction (10 μL) was suspended and incubated, at 37°C in the dark, in 1 mL of a solution composed by 30% PBS, 1 mM $CaCl_2$, 1 mM $MgCl_2$, 1% of 10 mM Tris-150 mM NaCl buffer (pH 8) and 1 mM L-Ala 4-Nitroanilide. At the same time, two standard solutions of 4-Nitroaniline (10 and 100 μM) were prepared using the same buffer. The reaction was stopped, maintaining samples at 4°C for 10 min. The absorbance of each sample was evaluated at 405 nm and the formed 4-Nitroanilide μmoles were calculated using the standard curve. The APN-specific activity was expressed as mU/mg protein.

Transepithelial electrical resistance

Co-culture cells were seeded in a 24-well plate (Transwell Millicell Cell Culture Insert PET 1 μm, Millicell 24-Well Receiver Tray, Millipore Corporation, Billeric, MA, USA) and maintained in their growth medium until the measurement. For each sample, transepithelial electrical resistance (TEER) value represented the mean value of the measures obtained in three different regions of the well using a Millicell ERS system (Millipore Corporation). TEER was evaluated, at all the time points indicated for each protocol, either for the co-culture or in absence of cells (blank), and this latter measure was then subtracted to all the cell values. TEER values were expressed as $\Omega\ cm^2 \times 10^5$ cells, this format takes into account the different co-culture proliferation rates of the three protocols.

Lucifer Yellow permeability study

Lucifer yellow (LY) was used to evaluate the co-culture paracellular permeability to large molecules at T6 and T15, for each protocol. Cells were seeded and maintained in a 24-well plate (Transwell Millicell Cell Culture Insert PET 1 μm, Millicell^R 24-Well Receiver Tray, Millipore Corporation) in complete RPMI.

For each well, after removing the medium, a solution of 100 μM LY in Hank's Balance Salt Solution (HBSS) was added at the apical chamber and cells were incubated for 120 min. At the end of the incubation period, both apical and basolateral solutions were collected and the emitted fluorescence was detected at $\lambda_{excitation}$ = 398 nm and $\lambda_{emission}$ = 518 nm by a luminescence spectrometer (Perkin Elmer, Beaconsfield, UK). Co-culture permeability results were expressed as the apparent permeability coefficient (P_{app}), which was calculated as follows:

S is the surface area of the membrane (0.7 cm^2), C_0 is the initial concentration of LY in the apical compartment, Q is the amount of LY molecules transported from the apical to basolateral chamber in a specific time period (t = 120 min).

Determination of NO production

The co-culture NO production, at each time point of the three protocols, was evaluated by the fluorescent probe diaminofluorescein-FM diacetate (DAF-FM DA), as described previously [29,30] with some modifications. Cells were seeded into a 96-well black plate (Greiner bio-one Cellstar) in complete RPMI. The day of the experiment, the growth medium was removed, cells were washed with PBS, and finally incubated with 40 μM DAF-FM DA in HBSS solution (with 10 mM Hepes) for 1 h. After incubation, fluorescence ($\lambda_{excitation}$ = 500 nm; $\lambda_{emission}$ = 515 nm) was measured immediately and after 120 min by a Wallac Victor^2 1420 Multilabel Counter plate reader (Perkin Elmer). Results obtained were expressed as the average daily production of NO $\times 10^5$ cells, calculated as reported in 2.15 paragraph, to consider the different co-culture proliferation rates and the different timing of medium administration of the three protocols.

Table 1
Semiquantitative analysis of ultrastructural features of 70/30 Caco2/HT-29 co-culture for the ST, IN, and EX conditions in relation with days in culture

	T3	T7	T11	T15
Multilayer				
ST	+	+	+	++
IN	±	+	±	+
EX	+	+	+	±
Microvilli				
ST	±	+	±	++
IN	±	+	±	±
EX	–	+	±	±
Cell junctions				
ST	±	+	±	++
IN	±	++	–	+
EX	–	+	±	–
Follicle-like structures				
ST	–	+	±	+
IN	±	±	++	+
EX	+	+	+	++

EX, excess; IN, intermediate; ST, standard

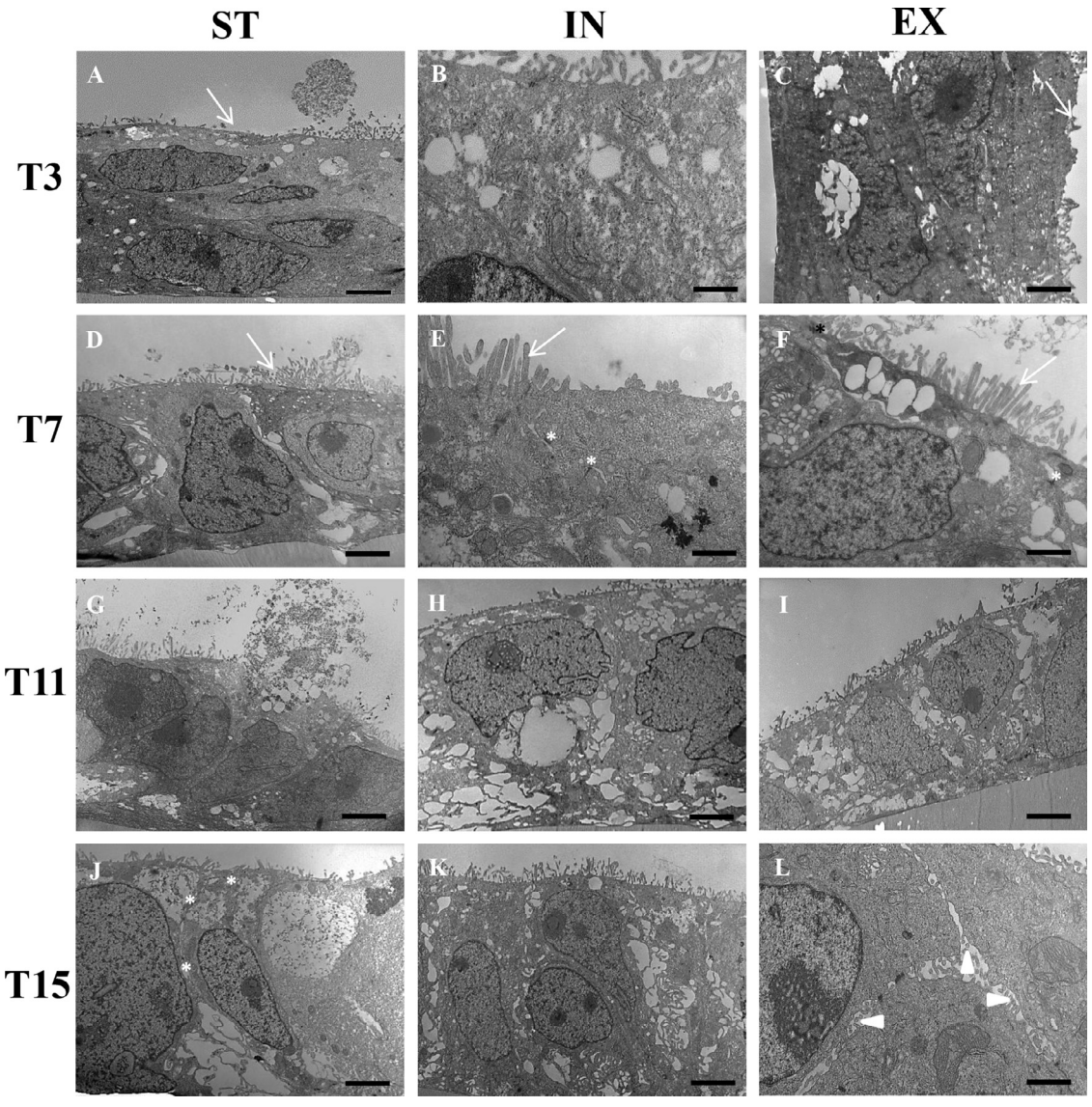

Fig. 2. TEM microphotographs of co-culture adapted to ST, IN, and EX medium change protocols with days in culture. Ultrathin araldite sections of co-culture. (**A**–**C**) T3 cells. (**D**–**F**) T7 cells; (**G**–**I**) T11 cells, and (**J**–**L**) T15 cells. EX, excess; IN, intermediate; ST, standard; TEM, transmission electron microscopy. Black arrows: Microvilli; asterisks: cell junctions; arrowheads: follicle-like structures. Bars 2 μm, except for B: bar 500 nm.

Determination of ROS production

The ROS production evaluation was performed using the cell antioxidant activity assay, based on the use of the fluorescent probe 2′,7′-dichlorofluorescin diacetate, as described previously [31] with some modifications. Co-culture cells were seeded into a black 96-well plate (Greiner bio-one Cellstar) in complete RPMI. At the desired time point, the growth medium was removed, cells were washed with PBS and, subsequently, cells were incubated with 60 μM 2′,7′-dichlorofluorescin diacetate in HBSS solution (with 10 mM Hepes) for 20 min. After incubation, the fluorescence ($\lambda_{excitation}$ = 485; $\lambda_{emission}$ = 538) was measured immediately and after 120 min by a Wallac Victor^2 1420 Multilabel Counter plate reader (Perkin Elmer). Results obtained after 120 min were expressed as the average daily production ROS × 10^5 cells, calculated as reported in the statistical analysis section, to consider the different co-culture proliferation rates and the different timing of medium administration of the three protocols.

IL-6, IL-8, and PYY anorectic hormone production

Co-culture was seeded in a 75 cm^2 Flasks (Greiner bio-one Cellstar) in complete RPMI. At each time point of the three protocols, cell medium was collected, centrifuged, and conserved at −80°C. The collected medium was used to measure the concentration of IL-6, IL-8, and PYY released by cells. The evaluation of IL-6 and IL-8 was performed using a magnetic luminex performance assay, whereas for PYY was performed using an enzyme-linked immunosorbent assay by LABOSPACEs.r.l. (Via Ranzato 12 – 20128 Milano, Italy). Results obtained were expressed as the average daily production of IL-6, IL-8, and PYY × 10^5 cells, calculated as reported in the next section, to consider the different co-culture proliferation rates and the different timing of medium administration of the three protocols.

Statistical analysis

Results shown in Figures 4 to 8 represent the mean values ± standard deviation (SD) from three independent experiments, each of them consisting of at least three replicates. In the case of Figure 7 (ROS and NO production) and Figure 8 (IL-6, IL-8, and PYY production), the mean values obtained by the experimental procedures (Arbitrary Units of Fluorescence (AUF) and picograms (pg), respectively) were normalized according to the following formula:

$$\text{Production by } 10^5 \text{ cells} = \frac{Mean\ (AUF\ or\ pg)}{cell\ number\ in\ the\ growth\ area\ of\ each\ experimental\ condition} \times 10^5$$

The production by 10^5 cells thus calculated was then divided by the number of days the growth medium remain in contact with cells before each time point: 4 in the case of ST; 2 in the case of IN, and 1 in the case of EX, to obtain the average daily production × 10^5 cells.

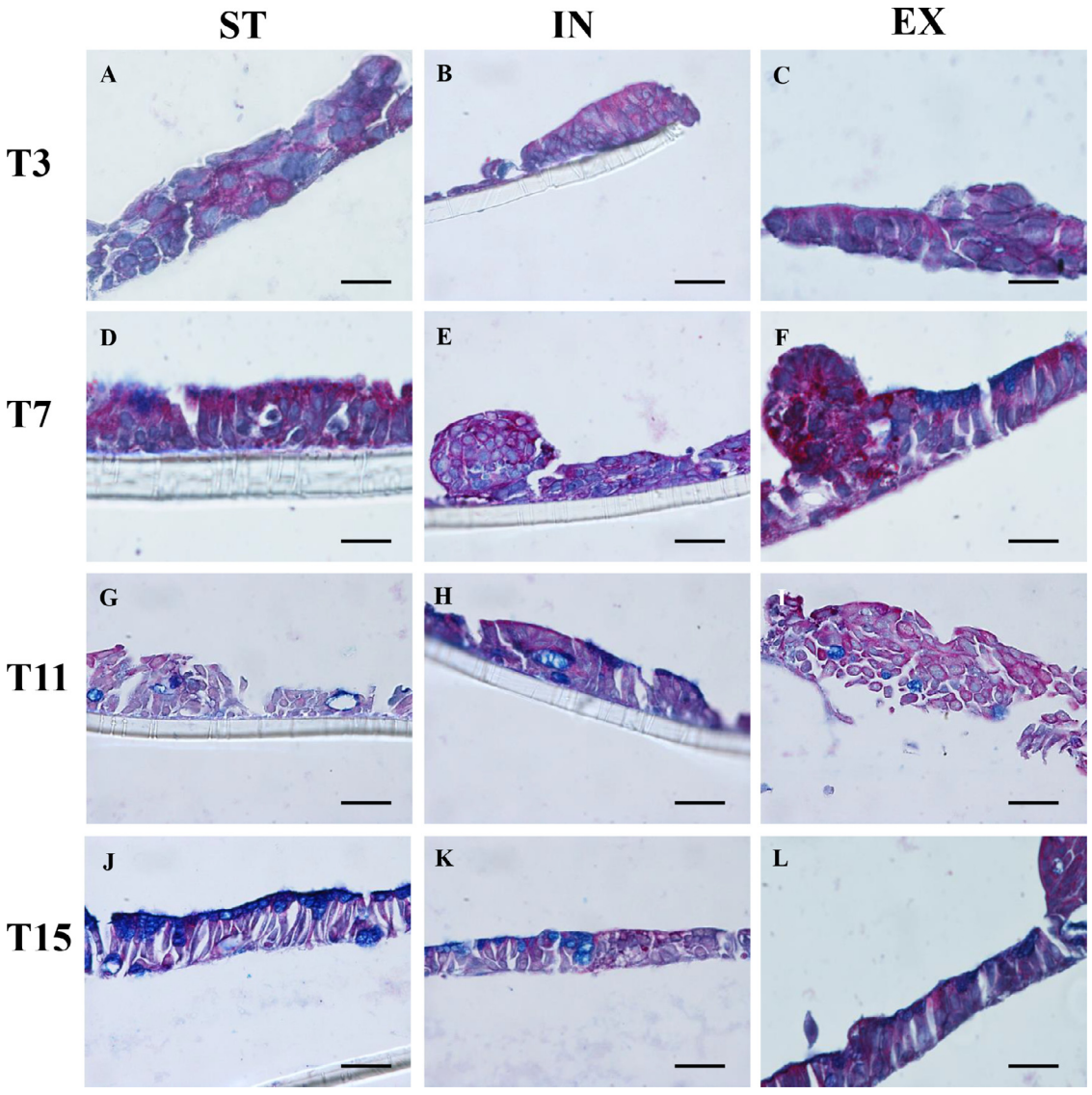

Fig. 3. Mucus presence in co-culture paraffin sections after PAS/Alcian Blue staining for ST, IN, and EX medium-change protocols with days in culture. (**A**–**C**) T3 cells. (**D**–**F**) T7 cells; (**G**–**I**) T11 cells, and (**J**–**L**) T15 cells. EX, excess; IN, intermediate; ST, standard. Bars 50 μm.

Statistically significant differences between mean values were established by one-way analysis of variance followed by a Bonferroni post hoc *t* test with the SPSS 20 statistical software (SPSS, Chicago, IL, USA). $P < 0.05$ was considered significant and was represented by different letters for intrasubject test (within the same protocol but at different time points) or symbols for intersubject test (between the three protocols at the same time point).

Results

Morphologic features

From T3, a multilayer was observed by transmission electron microscopy in all the experimental groups at a different degree for each experimental time point (Table 1). In ST, a multilayer was present at all time points (Fig. 2A,D,G,J). This spatial organization was less evident and comparable between IN and EX than in ST at T3 (Fig. 2 B,C), T7 (Fig. 2E,F), T11 (Fig. 2H,I), and in particular at T15 (Fig. 2K,L), suggesting a negative correlation with the nutrient excess at long time points.

At T3, the microvilli were scattered and not well developed in all experimental groups (Fig. 2A–C, see white arrows), whereas at T7, a clear absorptive phenotype with a brush border was present and comparable among groups (Fig. 2D–F, see white arrows). Afterward, the microvilli length and density tended to progressively diminish in all experimental groups, although to a different degree in each group (Fig. 2G–L). A similar trend was observed for the intercellular junctional apparatus, which was more evident from T3 to T7 (Fig. 2D–F, asterisks), whereas at T11, it declined in all experimental groups. Interestingly, at T15, cellular junctions were present to a great extent only in ST, to a lesser extent in the IN group, and absent in EX group (see Table 1 and asterisks in Fig. 2). Follicle-like structures (FLS) were particularly evident in the IN group at T11 (data not shown) and at T15 in the EX group (Fig. 2L, arrowheads).

The presence of mucus after PAS/Alcian Blue staining is reported in Figure 3. The reddish-violet staining indicates the mucus-producing cells and the presence of mucus, whereas the bluish cytoplasmic background indicates a non–mucus-secreting cell type [14]. Few mucus secreting cells were detected in all the three experimental groups at T3 (Fig. 3A–C), with a considerable increase at T7 (Fig. 3D–F). At T11 mucus was more evident in the

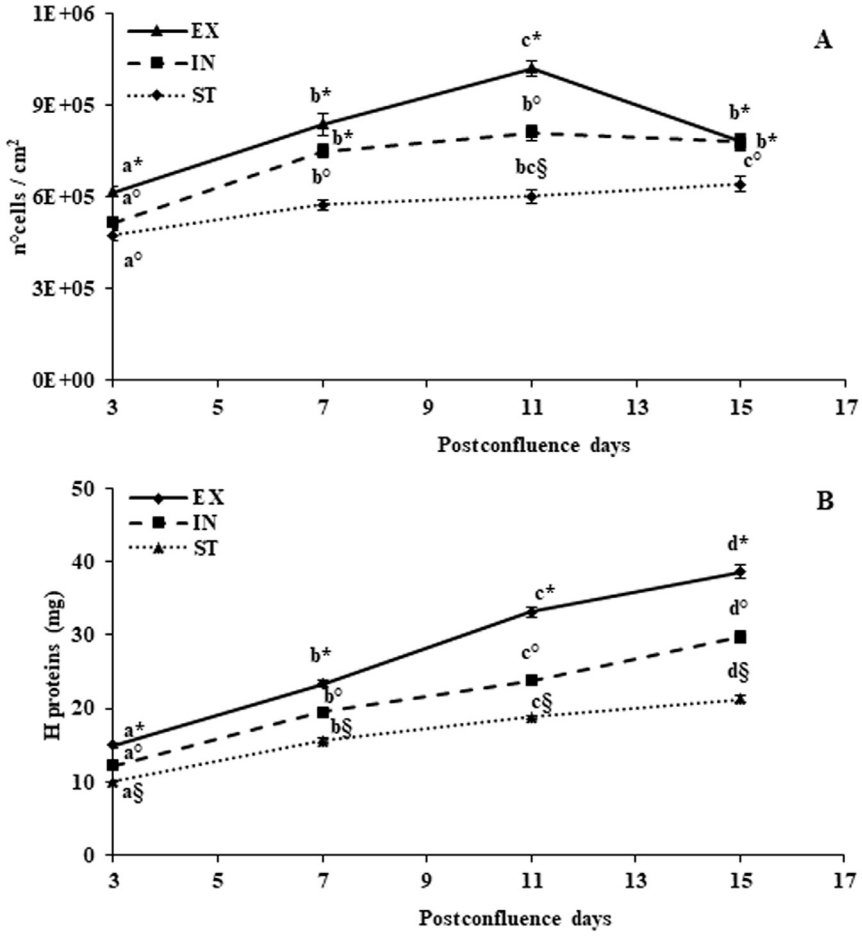

Fig. 4. Variation in cell number and protein content in the ST, IN, and EX medium-change protocols with days in culture. (**A**) Number of cells in 1 cm^2 growth area. (**B**) Protein content (mg) in the homogenates (H) of the different conditions. Data reported represent the mean ± SD of three independent experiments. Significant statistical differences are marked with different letters within the same protocol but at different time points ($P < 0.01$). Symbols indicate any statistical significant difference between the three protocols at the same time point ($P < 0.01$). EX, excess; IN, intermediate; SD, standard deviation; ST, standard.

IN (Fig. 3H) and in the EX groups (Fig. 3I) than in the ST group (Fig. 3G). At T15 mucus was virtually absent in ST (Fig. 3J), decreased in IN (Fig. 3), and was alike in EX (Fig. 3L).

Cellular features

Cell number increased with days in culture for all the growth conditions with slight differences, reaching a plateau at T7 in the case of ST and IN and at T11 in the case of EX. After that time, it dropped to the IN value at T15, probably because the insufficient growth area for cells to further proliferate. The cell number was always significantly higher in EX and IN than in ST (Fig. 4A). Cell number in the IN condition was significantly higher than ST from T7 on T15. Analogously, the protein density increased with days in culture in all the growth conditions and it was always significantly higher in IN than ST condition and in the EX than ST and IN conditions (Fig. 4B). The level of significance among all the comparisons was $P < 0.01$.

Enzyme activities

The IN and EX conditions induced an increase in ALP activity from T3 to T15, whereas the ST condition induced an increase until T11. ALP activity for the EX condition was always higher than in the IN and ST conditions at all postconfluence days but in particular at T11 and T15 (Fig. 5A). APN activity increased in the ST condition only at T15, whereas in the IN and EX conditions it increased from T3 to T15 (Fig. 5B). All the growth conditions determined an increase in the DPP-IV activity; however, differently from the previous enzymes, the values were higher in the ST group than in the IN and EX groups. EX values were always the lowest (Fig. 5C). This trend reflects the cell exposure to increasing concentration of the amino acids Met, Leu, and Trp, known inhibitors of the DPP-IV activity, although without reaching a suppression. The level of significance among all the comparisons was $P < 0.01$ except for APN values between EX and IN at T3 ($P < 0.05$).

Permeability features

TEER values in the ST group remained almost constant with days in culture. In the IN group, TEER values decreased at T7 to form a plateau. In the EX condition, they decreased at T11 and then slightly returned to T3 values (Fig. 6A; $P < 0.05$). LY P_{app} evaluation showed values significantly different only at T15, where they were higher in EX than in the ST and IN conditions (Fig. 6B; $P < 0.01$).

Oxidative status

ROS production was always higher in the EX condition than in the ST and IN conditions at all postconfluence days (Fig. 7A),

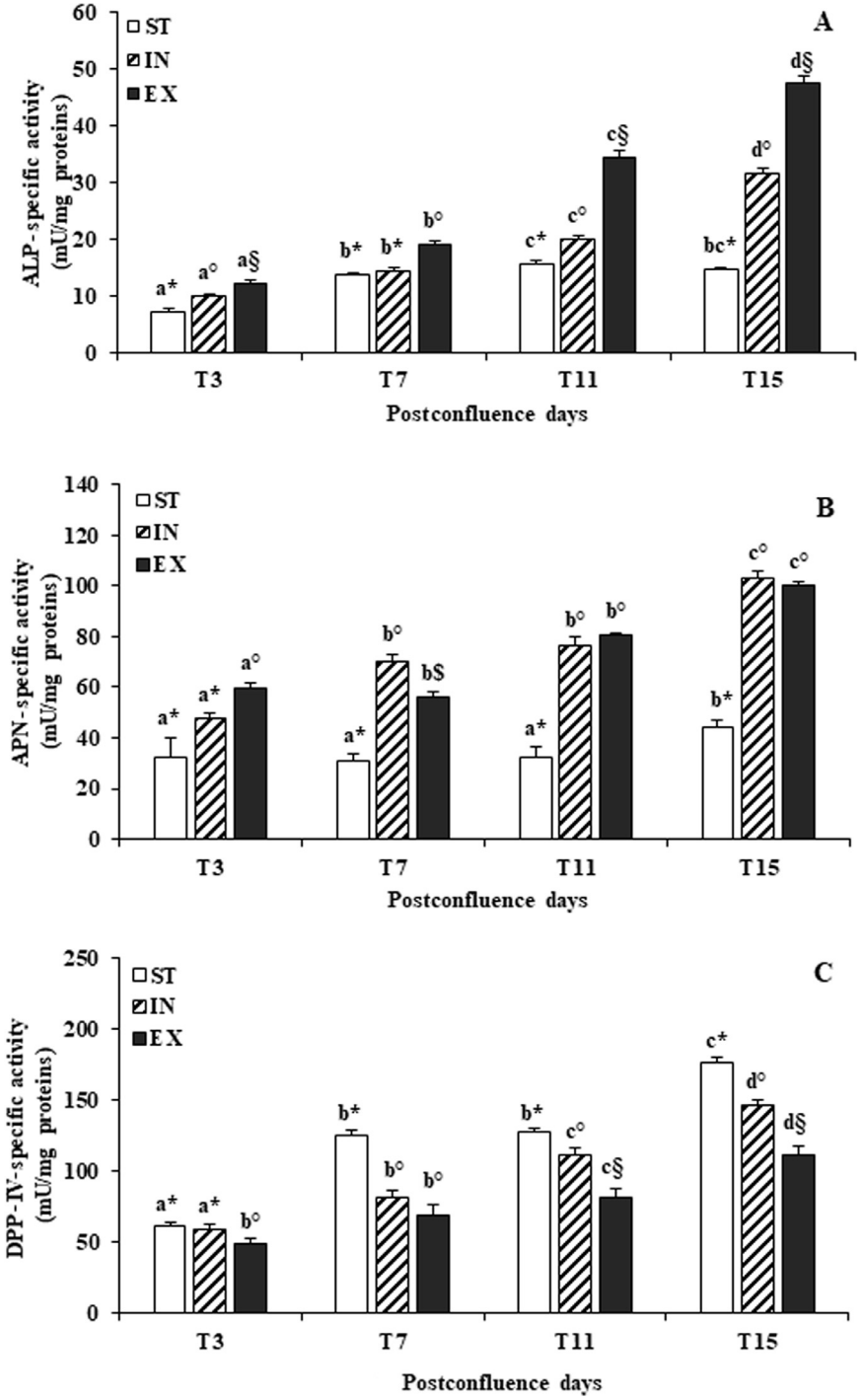

Fig. 5. Enzyme-specific activity for ST, IN, and EX medium-change protocols with days in culture. (**A**) ALP activity; (**B**) APN activity; (**C**) DPP-IV activity. Data reported represent the mean ± SD of three independent experiments. The reported specific activity was measured on P2 cell fraction containing membranes and microvilli. Enzyme units were expressed as reported in the method section. Significant statistical differences are marked with different letters within the same protocol but at different time points. Symbols indicate any statistical significant difference between the three protocols at the same time point. The level of significance among all the comparisons was $P < 0.01$ except for APN values between EX and IN at T3 ($P < 0.05$). ALP, alkaline phosphatase; APN, aminopeptidase N; DPP-IV, dipeptidyl peptidase-IV; EX, excess; IN, intermediate; SD, standard deviation; ST, standard.

whereas IN values were only modestly higher than ST values. The latter values did not significantly differ with days in culture, thus underlying the full viability of the co-culture till the end of the experiment. The level of significance was $P < 0.01$ among all samples except, for the variation in IN and ST along with the postconfluence. On the contrary, NO production in the EX condition reached the highest value at T3 and then decreased, although the value remained always higher than the ST and IN conditions. The decreasing trend was also observed in the IN condition (Fig. 7B). The level of significance was $P < 0.01$ among all the comparisons, except between T7 and T11 for IN ($P < 0.05$).

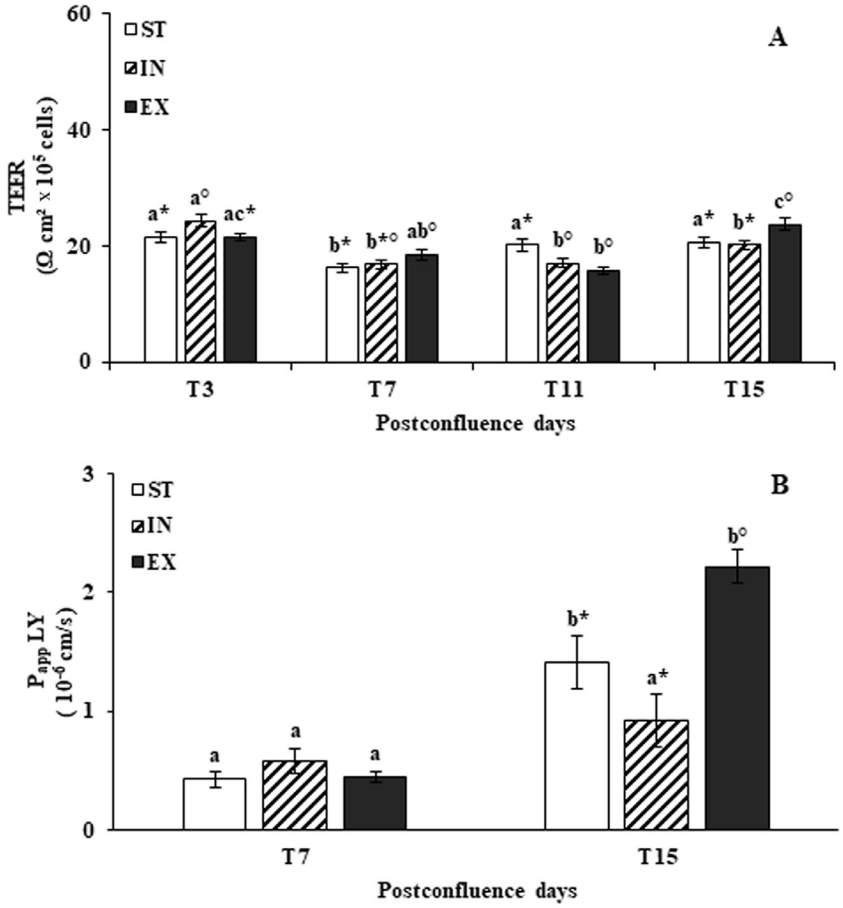

Fig. 6. Permeability indexes for ST, IN, and EX medium-change protocols with days in culture. (**A**) TEER measurements; (**B**) Lucifer yellow P_{app} evaluation. Data reported represent the mean ± SD of three independent experiments. TEER values were normalized for 10^5 cells. Significant statistical differences are marked with different letters within the same protocol condition but at different time points. Symbols indicate any statistical significant difference between the three protocols at the same time point. The level of significance was $P < 0.05$ in the case of TEER values and $P < 0.01$ in the case of P_{app} values. EX, excess; IN, intermediate; SD, standard deviation; ST, standard; TEER, transepithelial electrical resistance.

Inflammation degree and PYY anorectic hormone production

IL-6 production was always higher in the EX condition than in the ST and IN condition at all postconfluence days, although the EX values did not significantly vary with the postconfluence (Fig. 8A). The IL-6 values for the IN and ST conditions never differed with time in culture. IL-8 production was significantly higher for all the conditions only at T15 and, at this time point, the EX value was the highest (Fig. 8B). The level of significance was $P < 0.01$ among all the comparisons and for both IL-6 and IL-8, except between IN and EX at T11 ($P < 0.05$).

PYY was definitely higher in the EX condition than in the ST and IN conditions at all the postconfluence days considered (Fig. 8C). The level of significance was $P < 0.01$ among all the comparisons.

Discussion

To our knowledge, the published in vitro studies on intestinal cell differentiation and function have considered the composition of growth medium, the growth cell support, and the presence of cell differentiation inducers [32]. In vitro cultures of intestinal cells from cancer origin are particularly susceptible to some components of the growth medium, such as glucose or galactose and glutamine [33]. Conversely, no studies are available on the role of intestinal differentiated cells of the higher frequency of medium change, thus an excess of nutrients.

The present study represented the first report on the morphofunctional modifications induced by an excess of nutrients administered by means of higher frequency medium changing compared with a standard procedure in a human intestinal in vitro cell model. Altogether, data presented here showed that an excess of nutrients in a co-culture in vitro intestinal model induced morphofunctional adaptations similar to those reported by in vivo studies and related to the developing of an obese phenotype. From the morphologic point of view, the ST condition always showed a multilayered arrangement of the co-culture, as previously reported [13]—more evident than in the IN and EX groups and particularly marked at T15. This was in agreement with most of the reported methods set up to differentiate intestinal cells, from the original [34] to the most recent ones [35,36]. Similarly, in the ST group the absence of mucus as revealed by PAS/Alcian blue staining stands for an epithelium with a prevalent absorptive phenotype.

In the co-culture fed with an excess of nutrients, an increase in the proliferation rate was observed but, differently from in vivo studies [3], it was due to well-differentiated intestinal cells (i.e., enterocytes and mucus-secreting cells). An increased paracellular permeability was similarly observed, as shown by the increase of the LY P_{app} at T15, and seemed to be caused by the disappearance of the tight junctions instead of a different protein modulation as

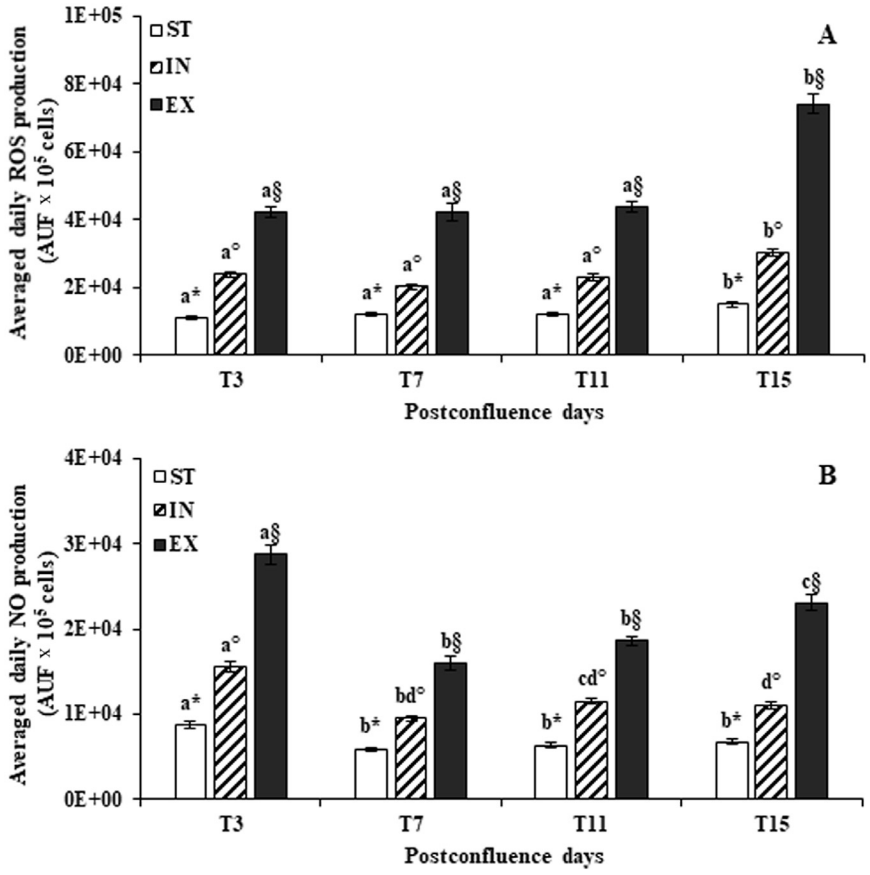

Fig. 7. Averaged daily ROS (**A**) and NO (**B**) production in ST, IN, and EX medium-change protocols with days in culture. Data reported are the mean ± SD from three independent experiments and were normalized as described in the statistical analysis section. Significant statistical differences are marked with different letters within the same protocol condition but at different time points. Symbols indicate any statistical significant difference between the three protocols at the same time point. The level of significance for ROS production was $P < 0.01$ among all samples except for the variation in the IN and ST conditions with time in culture ($P < 0.05$). The level of significance of NO production was $P < 0.01$ among all the comparisons except between T7 and T11 in the case of the IN condition ($P < 0.05$). EX, excess; IN, intermediate; ROS, reactive oxygen species; SD, standard deviation; ST, standard

reported by in vivo studies [6]. After transmission electron microscopy analysis, we can hypothesize that the disappearance of all intercellular junctions in EX at T15 is linked to the presence of intercellular spaces on the lateral membrane containing abundant microvilli. On the whole, these ultrastructural features associated with the higher amount of the substrates for ALP and APN, caused by frequent medium changes in the EX condition, can contribute to the higher enzymatic activity in the experimental setting, in accordance with in vivo experiments [7,10,11,37–40]. In the case of DPP-IV, the presence of inhibitors such as Met, Leu, and Trp, in the growth medium was responsible for its lower activity in the EX condition than in the ST and IN conditions.

Different studies have also shown that Caco2 and HT-29 cells were able to increase the production and the release of proinflammatory cytokines (IL-8, IL-6, and TNF-α) after the exposition to an inflammatory stimulus, such as lipopolysaccharide (LPS) and other inflammatory cytokines (TNF-α and IL-1) [41,42]. Moreover, in vivo studies have shown that the excess of some nutrients, such as long-chain fatty acids, is able to induce the onset of an inflammatory response by the intestinal epithelium, caused by the production of proinflammatory cytokines or free radicals by the same intestinal epithelial cells [12,43,44]. The same effect was revealed in our in vitro intestinal model because the production of IL-6, IL-8, ROS, and NO in the EX condition was always the highest at each time point, underlining the onset of an inflammatory state in presence of a nutrient excess according to the results obtained by in vivo studies.

It is worth underlining that the results obtained with the EX protocol here adopted were not always confirmed in the IN protocol, which gave only a modestly increased enzyme activity and permeability and almost no significant increase in cytokine production, a condition associated with a lower degree of ROS production than EX protocol and similar to the ST protocol. On the other hand, in IN samples, FLS presence was evident already at T11, which is earlier than in the EX group, but yet at T15 declined, underlying that the IN condition represents a transitory state in relation to the culture feeding. This consideration, together with the observation that the EX protocol almost always needed 15 d of postconfluence to reach the modifications, indicate that morphofunctional adaptation was reached only by a continuous high provision of nutrients for a long time.

Conclusions

There are two main outcomes of the present study: first, it serves as a guide to standardize, as far as possible, the intestinal cell growth with timely defined medium changes to minimize any not required variation in the morphofunctional features which could be able to affect reproducibility in cell studies. Second, it provides a useful in vitro intestinal cell model to understand the role of nutrient excess in the development of some of the pathologic mechanisms on which the obese phenotype is based.

The analogy between results obtained in in vivo animal models and in the present in vitro co-culture accounts for considering our

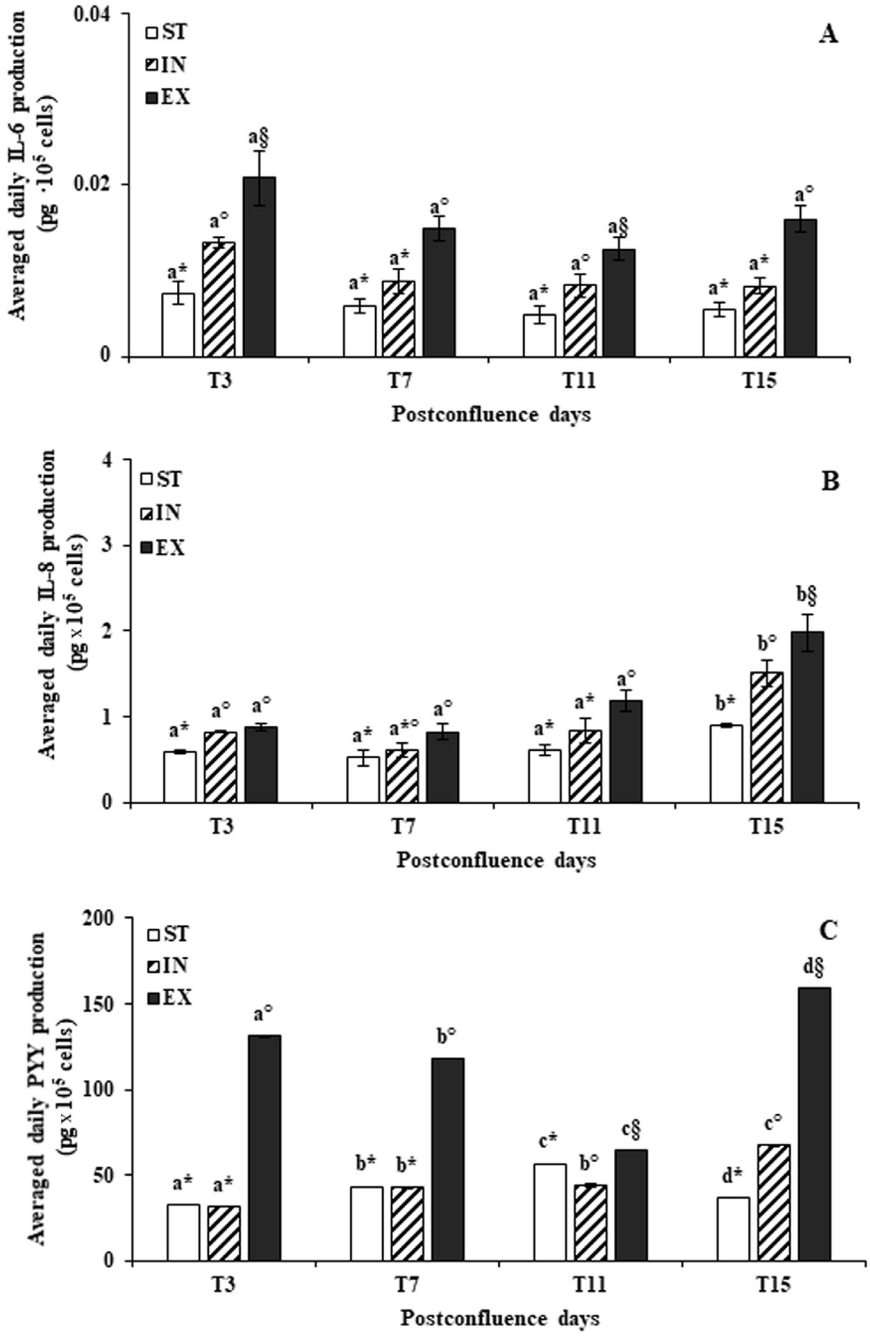

Fig. 8. Cytokine and PYY production in ST, IN, and EX medium change protocols with days in culture. (**A**) IL-6; (**B**) IL-8; (**C**) PYY. Data reported are the mean ± SD from three independent experiments and were normalized as described in the statistical analysis section. Significant statistical differences are marked with different letters within the same protocol condition but at different time points. Symbols indicate any statistical significant difference between the three protocols at the same time point. The level of significance was $P < 0.01$ among all the comparisons except between IN and EX at T11 in the case of IL-6 and IL-8 ($P < 0.05$). EX, excess; IL, interleukin; IN, intermediate; PYY, peptide YY; SD, standard deviation; ST, standard.

experimental set up to evaluate the molecular pathways involved in obesity and in obesity-associated pathologies instead of using animals. Although these pathologies are based on multifactorial components, the nutrient amount and specifity are the main determinants of the differences accounted between lean and obese individuals [45]. In fact, in the obese phenotype, the increased intestinal absorption [5] and permeability [12], together with a modification in hormone secretion, are caused by hyperphagia rather than body weight and systemic factors [45]. All these changes represent an adaptation of the gut to an excess of nutrients.

The next step will be to set up a complete obese in vitro intestinal co-culture cell model with the presence of the different intestinal microbiome associated with lean and obese phenotype to better understand the intestinal and nutrient absorption modifications and their effect on cell differentiation and function.

Acknowledgments

The authors acknowledge Marianna Gaman for transmission electron microscopy technical support.

References

[1] Shimizu M. Interaction between food substances and the intestinal epithelium. Biosci Biotechnol Biochem 2010;74:232–41.
[2] Mao J, Hu X, Xiao Y, Yang C, Ding Y, Hou N, et al. Overnutrition stimulates intestinal epithelium proliferation through β-catenin signaling in obese mice. Diabetes 2013;62:3736–46.
[3] Mah AT, Van Landeghem L, Gavin HE, Magness ST, Lund PK. Impact of diet-induced obesity on intestinal stem cells: hyperproliferation but impaired intrinsic function that requires insulin/IGF1. Endocrinology 2014;155:3302–14.
[4] Altmann GG, Leblond CP. Factors influencing villus size in the small intestine of adult rats as revealed by transposition of intestinal segments. Am J Anat 1970;127:15–36.
[5] Verdam FJ, Greve JW, Roosta S, van Eijk H, Bouvy N, Buurman WA, et al. Small intestinal alterations in severely obese hyperglycemic subjects. J Clin Endocrinol Metab 2011;96:E379–83.
[6] Brun P, Castagliuolo I, Di Leo V, Buda A, Pinzani M, Palù G, et al. Increased intestinal permeability in obese mice: new evidence in the pathogenesis of nonalcoholic steatohepatitis. Am J Physiol Gastrointest Liver Physiol 2007;292:G518–25.
[7] Sefcíková Z, Hájek T, Lenhardt L, Racek L, Mozes S. Different functional responsibility of the small intestine to high-fat/high-energy diet determined the expression of obesity-prone and obesity-resistant phenotypes in rats. Physiol Res 2008;57:467–74.
[8] Nongonierma AB, Mooney C, Shields DC, Fitzgerald RJ. Inhibition of dipeptidyl peptidase IV and xanthine oxidase by amino acids and dipeptides. Food Chem 2013;141:644–53.
[9] Lacroix I, Li-Chan E. Dipeptidyl peptidase-IV inhibitory activity of dairy protein hydrolysates. Int Dairy J 2012;25:97–102.
[10] King IS, Paterson JY, Peacock MA, Smith MW, Syme G. Effect of diet upon enterocyte differentiation in the rat jejunum. J Physiol 1983;344:465–81.
[11] Raul F, Goda T, Gossé F, Koldovský O. Short-term effect of a high-protein/low-carbohydrate diet on aminopeptidase in adult rat jejunoileum. Site of aminopeptidase response. Biochem J 1987;247:401–5.
[12] Ding S, Lund PK. Role of intestinal inflammation as an early event in obesity and insulin resistance. Curr Opin Clin Nutr Metab Care 2011;14:328–33.
[13] Ferraretto A, Bottani M, De Luca P, Cornaghi L, Arnaboldi F, Maggioni M, et al. Morphofunctional properties of a differentiated Caco2/HT-29 co-culture as an in vitro model of human intestinal ephitelium. Biosci Rep 2018;38: BSR20171497.
[14] Stuknyte M, Maggioni M, Cattaneo S, De Luca P, Fiorilli A, Ferraretto A, et al. Release of wheat gluten exorphins A5 and C5 during in vitro gastrointestinal digestion of bread and pasta and their absorption through an in vitro model of intestinal epithelium. Food Res Int 2015;72:208–14.
[15] De Luca P, Bruschi S, Maggioni M, Stuknytė M, Cattaneo S, Bottani M, et al. Gastrointestinal digestates of Grana Padano and Trentingrana cheeses promote intestinal calcium uptake and extracellular bone matrix formation in vitro. Food Res Int 2016;89(Pt 1):820–7.
[16] Hidalgo A, Ferraretto A, De Noni I, Bottani M, Cattaneo S, Galli S, et al. Bioactive compounds and antioxidant properties of pseudocereals-enriched water biscuits and their in vitro digestates. Food Chem 2018;240:799–807.
[17] Bottani M, Brasca M, Ferraretto A, Cardone G, Casiraghi MC, Lombardi G, et al. Chemical and nutritional properties of white bread leavened by lactic acid bacteria. J Funct Foods 2018;45:330–8.
[18] Maggioni M, Stuknyte M, De Luca P, Cattaneo S, Fiorilli A, De Noni I, et al. Transport of wheat gluten exorphins A5 and C5 through an in vitro model of intestinal epithelium. Food Res Int 2016;88:319–26.
[19] Ferraretto A, Gravaghi C, Donetti E, Cosentino S, Donida BM, Bedoni M, et al. New methodological approach to induce a differentiation phenotype in Caco-2 cells prior to post-confluence stage. Anticancer Research 2007;27:3919–25.
[20] Hekmati M, Polak-Charcon S, Ben-Shaul Y. A morphological study of a human adenocarcinoma cell line (HT29) differentiating in culture. Similarities to intestinal embryonic development. Cell Differ Dev 1990;31:207–18.
[21] Strober W. Trypan blue exclusion test of cell viability. Curr Protoc Immunol 2001. Appendix 3:Appendix 3 B.
[22] Schmitz J, Preiser H, Maestracci D, Ghosh BK, Cerda JJ, Crane RK. Purification of the human intestinal brush border membrane. Biochim Biophys Acta 1973;323:98–112.
[23] Zweibaum A, Pinto M, Chevalier G, Dussaulx E, Triadou N, Lacroix B, et al. Enterocytic differentiation of a subpopulation of the human colon tumor cell line HT-29 selected for growth in sugar-free medium and its inhibition by glucose. J Cell Physiol 1985;122:21–9.
[24] Lowry OH, Rosebrough NJ, Farr AL, Randall RJ. Protein measurement with the Folin phenol reagent. J Biol Chem 1951;193:265–75.
[25] Buras RR, Shabahang M, Davoodi F, Schumaker LM, Cullen KJ, Byers S, et al. The effect of extracellular calcium on colonocytes: evidence for differential responsiveness based upon degree of cell differentiation. Cell Prolif 1995;28:245–62.
[26] Morita A, Chung YC, Freeman HJ, Erickson RH, Sleisenger MH, Kim YS. Intestinal assimilation of a proline-containing tetrapeptide. Role of a brush border membrane postproline dipeptidyl aminopeptidase IV. J Clin Invest 1983;72:610–6.
[27] Hopus-Havus VK, Glenner GG. A new dipeptide naphthylamidase hydrolyzing glycyl-prolyl-β-naphthylamide. Histochemie 1966;7:197–201.
[28] Ferruzza S, Rossi C, Scarino ML, Sambuy Y. A protocol for in situ enzyme assays to assess the differentiation of human intestinal Caco-2 cells. Toxicol In Vitro 2012;26:1247–51.
[29] Viani P, Giussani P, Ferraretto A, Signorile A, Riboni L, Tettamanti G. Nitric oxide production in living neurons is modulated by sphingosine: a fluorescence microscopy study. Febs Letters 2001;506:185–90.
[30] Balcerczyk A, Soszynski M, Bartosz G. On the specificity of 4-amino-5-methylamino-2′,7′-difluorofluorescein as a probe for nitric oxide. Free Radical Biology and Medicine 2005;39:327–35.
[31] Wan H, Liu D, Yu X, Sun H, Li Y. A Caco-2 cell-based quantitative antioxidant activity assay for antioxidants. Food Chem 2015;175:601–8.
[32] Sambuy Y, De Angelis I, Ranaldi G, Scarino ML, Stammati A, Zucco F. The Caco-2 cell line as a model of the intestinal barrier: influence of cell and culture-related factors on Caco-2 cell functional characteristics. Cell Biol Toxicol 2005;21:1–26.
[33] Zweibaum A, Laburthe M, Grasset E, Louvard D. Use of cultured cell lines in studies of intestinal cell differentiation and funtion. In: Compr Physiol 2011, supplement 19: Handbook of Physiology, The Gastrointestinal System, Intestinal Absorption and Secretion: p. 223-255. First published in print 1991.
[34] Pinto M, Robine-Leon S, Appay MD, Kedinger M, Triadou N, Dussaulx E, et al. Enterocyte-like differentiation and polarization of the human colon carcinoma cell line Caco-2 in culture. Biol Cell 1983;47:323–30.
[35] Nollevaux G, Devillé C, El Moualij B, Zorzi W, Deloyer P, Schneider YJ, et al. Development of a serum-free co-culture of human intestinal epithelium cell-lines (Caco-2/HT29-5 M21). BMC Cell Biol 2006;7:20–30.
[36] Béduneau A, Tempesta C, Fimbel S, Pellequer Y, Jannin V, Demarne F, et al. A tunable Caco-2/HT29-MTX co-culture model mimicking variable permeabilities of the human intestine obtained by an original seeding procedure. Eur J Pharm Biopharm 2014;87:290–308.
[37] Lallès JP. Intestinal alkaline phosphatase: Multiple biological roles in maintenance of intestinal homeostasis and modulation by diet. Nutr Rev 2010;68:323–32.
[38] Millán JL. Alkaline phosphatases: structure, substrate specificity and functional relatedness to other members of a large superfamily of enzymes. Purinergic Signal 2006;2:335–41.
[39] Mozes S, Sefcíková Z, Lenhardt L, Racek L. Obesity and changes of alkaline phosphatase activity in the small intestine of 40- and 80-day-old rats subjected to early postnatal overfeeding or monosodium glutamate. Physiol Res 2004;53:177–86.
[40] Lallès JP. Intestinal alkaline phosphatase: novel functions and protective effects. Nutr Rev 2014;72:82–94.
[41] Kaulmann A, Legay S, Schneider YJ, Hoffmann L, Bohn T. Inflammation related responses of intestinal cells to plum and cabbage digesta with differential carotenoid and polyphenol profiles following simulated gastrointestinal digestion. Mol Nutr Food Res 2016;60:992–1005.
[42] Schuerer-Maly C-C, Eckmann L, Kagnoff MF, Falco MT, Maly F-E. Colonic epithelial cell lines as a source of interleukin-8: stimulation by inflammatory cytokines and bacterial lipopolysaccharide. Immunology 1994;81:85–91.
[43] Yoshida H, Miura S, Kishikawa H, Hirokawa M, Nakamizo H, Nakatsumi RC, et al. Fatty acids enhance GRO/CINC-1 and interleukin-6 production in rat intestinal epithelial cells. J Nutr 2001;131:2943–50.
[44] Ji Y, Sakata Y, Tso P. Nutrient-induced inflammation in the intestine. Curr Opin Clin Nutr Metab Care 2011;14:315–21.
[45] Dailey MJ. Nutrient-induced intestinal adaption and its effect in obesity. Physiol Behav 2014;136:74–8.